

Radiation Effects and Defects in Solids

Incorporating Plasma Science and Plasma Technology

ISSN: (Print) (Online) Journal homepage: <https://www.tandfonline.com/loi/grad20>

Investigation of good dopant (Sm, Cu, Tb, Mn, Sb) for radiation dosimetry in the γ -excited $\text{GdCa}_4\text{O}(\text{BO}_3)_3$ phosphor: mechanoluminescence study

G. C. Mishra, Upendra K. Verma & S. J. Dhoble

To cite this article: G. C. Mishra, Upendra K. Verma & S. J. Dhoble (2022): Investigation of good dopant (Sm, Cu, Tb, Mn, Sb) for radiation dosimetry in the γ -excited $\text{GdCa}_4\text{O}(\text{BO}_3)_3$ phosphor: mechanoluminescence study, Radiation Effects and Defects in Solids, DOI: [10.1080/10420150.2022.2116708](https://doi.org/10.1080/10420150.2022.2116708)

To link to this article: <https://doi.org/10.1080/10420150.2022.2116708>



Published online: 09 Sep 2022.



Submit your article to this journal [↗](#)



View related articles [↗](#)



View Crossmark data [↗](#)



Investigation of good dopant (Sm, Cu, Tb, Mn, Sb) for radiation dosimetry in the γ -excited $\text{GdCa}_4\text{O}(\text{BO}_3)_3$ phosphor: mechanoluminescence study

G. C. Mishra^a, Upendra K. Verma^a and S. J. Dhoble^b,

^aDepartment of Physics, OP Jindal University, Raigarh, India; ^bDepartment of Physics, R.T.M. Nagpur University, Nagpur, India

ABSTRACT

The mechanoluminescence (ML) of $\text{GdCa}_4\text{O}(\text{BO}_3)_3$: Sm, Cu, Tb, Mn, Sb are studied and synthesized by a solid-state reaction process. The section clarity, crystallinity and configuration of the material are established by XRD while the FTIR spectrum of the sample confirms its practical cluster $(\text{BO}_3)_3$ and phonon frequency of the molecules in the host. B-O triangle structure defines its constructional inflexibility. Photoluminescence (PL) of $\text{GdCa}_4\text{O}(\text{BO}_3)_3$ with dopants $\text{Cu}_{0.2\text{mol}\%}$, $\text{Mn}_{0.2\text{mol}\%}$, $\text{Tb}_{0.1\text{mol}\%}$, $\text{Sm}_{0.2\text{mol}\%}$, $\text{Sb}_{0.1\text{mol}\%}$ and its transition confirms the incorporation of dopant within the host material. The ready phosphor could also be vital for stress sensing applications and accidental radiation measurement as it responds linearly to γ -ray dose and impact rate of the piston is very less sensitive for lower exposure and also it has very low fading, on storage.

ARTICLE HISTORY

Received 14 February 2022
Accepted 13 August 2022

KEYWORDS


FTIR; solid-state reaction;
oxiborate;
Mechanoluminescence;
radiation dosimetry

1. Introduction

The phenomenon of mechanoluminescence (ML) conjointly called piezo, fracto and triboluminescence (1–9) has generated wide-ranging analysis interest in recent years owing to its potential application for damage detection, self-diagnosis, optical stress sensors for recording defects and damages, fuse system for army warheads, time visualizations of stress distribution in solids, stress field close to crack-tip, and additionally for developing a safety-monitoring network system, foretelling of the associate earthquake, to detect sudden fracture of ceramic construction. Almost five-hundredths of crystal multifarious exhibit a range of ML (10–19).

The mechano-luminescence could be a classical phenomenon that is exposed when light is emitted by a phosphor sample (solid) once it is more experienced some process of deformation like cutting, shaking, rubbing, or dropping of loads on the sample (20).

Earlier because of the weak, non-reproducible and damaging nature of the ML emission, it attracted academicians solely and failed to ensue in any course of application, however, today, the impact of radiation has become vital because of its influence in numerous areas like radiation drugs, radiation therapy, food process, radiation-based chemical process and

CONTACT Upendra K. Verma  upendra4870@gmail.com

non-destructive testing techniques victimization radiography. Competent radiation measure mechanisms need to be advanced over a good variety of dose proportions. Up to now, several efforts are taken to hunt for new and high-performance thermoluminescence materials except for the increasing want for measure materials utilized in the surroundings, personal, and clinical radiation protection a lot of study on mechanoluminescence material is needed.

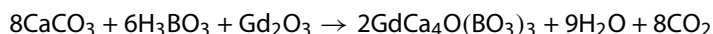
The thermoluminescence (TL) studies of borate compounds like BaB₄O₇: metal, Li₂B₄O₇:Cu, In, SrBa₄O₇:Dy, MgB₄O₇: Dy, Na, Ba₂Ca(BO₃)₂:Tb, Sr₂Mg (BO₃)₂ are enticing as a result of their close to tissue-equivalent integration constant and are reported pretty much as good TL materials (21–30). A replacement series of calcium-containing rare-earth oxyborates are synthesized and showed is structural with the composition of LnCa₄O(BO₃)₃ (Ln = La, Sm, Nd, Gd, Er, Y) and has area cluster monoclinic, non-centrosymmetric. These phosphors exhibit sensible thermal and chemical stability (31, 32).

Some of the TL materials also explain prominent ML peaks (33), this fact motivates us for the ML characterization. Phosphor shows ML intensity by any mechanical means like grinding, cleaving or scratching. An outsized range of researchers, particularly, in the Republic of India, China, and Japan square measure engaged in developing stress sensing techniques (34–38).

Mechanoluminescence also plays a vital role in radiation dosimetry as well as in sensor applications (14–19). Most of the researchers emphasize thermoluminescence and photoluminescence characterization of the phosphor and very less attention has been given to the mechanoluminescence (ML) study of the calcium-containing oxyborates. Within the gift article, we have got according to ML characterization of GdCa₄O(BO₃)₃ phosphors amalgamated by solid-state reaction methodology to grasp its importance for radiation measuring applications which shows the novelty of this work.

2. Synthesis details

The GdCa₄O(BO₃)₃ with completely different dopants (Sm, Cu, Tb, Mn, Sb) were ready by a solid-state reaction method at high temperatures. Raw materials were Gadolinium oxide, Calcium Carbonate, Boric Acid, Antimony trioxide (all are A.R., Himedia), Cupric Oxide, Samarium Oxide, Manganese Dioxide (all are Extra Pure, LOBA), Terbium Oxide (99.9% purity, Sigma Aldrich). A stoichiometric ratio of all the raw materials was beached systematically followed by heat at around 750°C intended for 10 h and after that frozen gradually Again these samples were grounded and fired at 850°C for another 10 h then cooled. The same process was repeated with different concentrations (0.05 to 1 mol%) of dopants (CuO, Sb₂O₃, Sm₂O₃, MnO₂, Tb₂O₃). The chemical reaction is:



To check the XRD patterns of the GdCa₄O(BO₃)₃ with the slandered pattern, an X-ray diffractometer (PW-1710) was adapted to record X-ray diffraction. A spectrofluorometer (Maruteck-FL-100-HS) is engaged to live the photoluminescence (PL) of the doped samples. By draping a load from a specific height onto a sample mounted on a Lucite plate with varied impact velocities utilizing a guiding metallic cylinder, ML is stimulated spontaneously. A 931A photomultiplier tube is located below the Lucite plate and associated to a storage oscilloscope to examine the luminescence (SM-340).

3. Results and discussions

3.1. XRD analysis

The condition of phase clarity and crystallinity of the ready sample $\text{GdCa}_4\text{O}(\text{BO}_3)_3$ was examined by an X-ray diffractometer (Figure 1) and therefore the pattern reveals that each one of the optical phenomenon peaks (d spacing shown in Chart 1) may be well indexed to the simulated XRD pattern of standard XRD shape of $\text{GdCa}_4\text{O}(\text{BO}_3)_3$ (JCPDS File no.89-1315).

3.2. SEM measurements

The SEM images of Sm, Cu, Tb, Mn and Sb doped $\text{GdCa}_4\text{O}(\text{BO}_3)_3$ phosphors with different resolutions are shown in Figure 2(a–e). All the samples are irregular shapes and average crystallite size in the micrometer range as grain morphology is destroyed due to grinding. The particles seem to be aggregated to each other during synthesis.

3.3. FTIR measurements

Figure 3 shows the FTIR spectra of $\text{GdCa}_4\text{O}(\text{BO}_3)_3$. BO_3 group functions as the central structural units in B-O triangles within the crystal structure of $\text{GdCa}_4\text{O}(\text{BO}_3)_3$, which provides

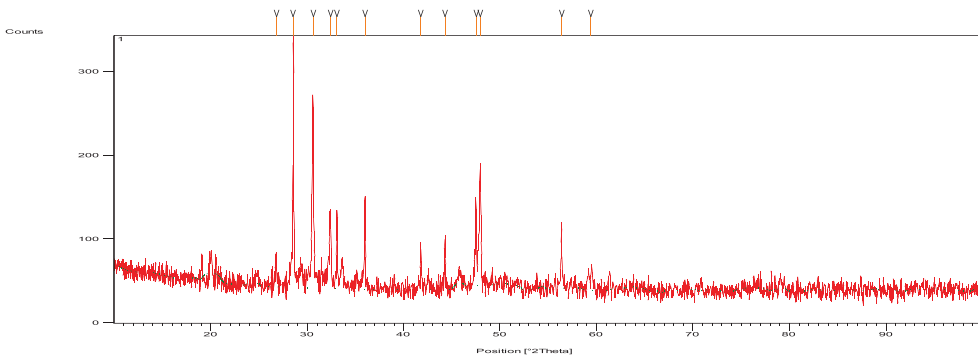


Figure 1. XRD pattern of $\text{GdCa}_4\text{O}(\text{BO}_3)_3$ crystal.

Pos. [°2Th.]	Height [cts]	FWHM [°2Th.]	d-spacing [Å]	Rel. [%]	Int.
26.7735	36.73	0.2448	3.32709	12.14	
28.5335	302.54	0.1020	3.12575	100.00	
30.5907	230.05	0.1020	2.92007	76.04	
32.3979	93.54	0.2040	2.76119	30.92	
33.0921	94.97	0.1224	2.70484	31.39	
35.9719	108.42	0.1224	2.49462	35.84	
41.8020	39.19	0.2448	2.15919	12.95	
44.2644	59.11	0.1224	2.04462	19.54	
47.4998	97.07	0.1224	1.91262	32.08	
47.9388	147.30	0.1632	1.89613	48.69	
56.3575	65.12	0.1632	1.63122	21.52	
59.3665	14.87	0.6528	1.55552	4.91	

Chart 1. Peak positions.

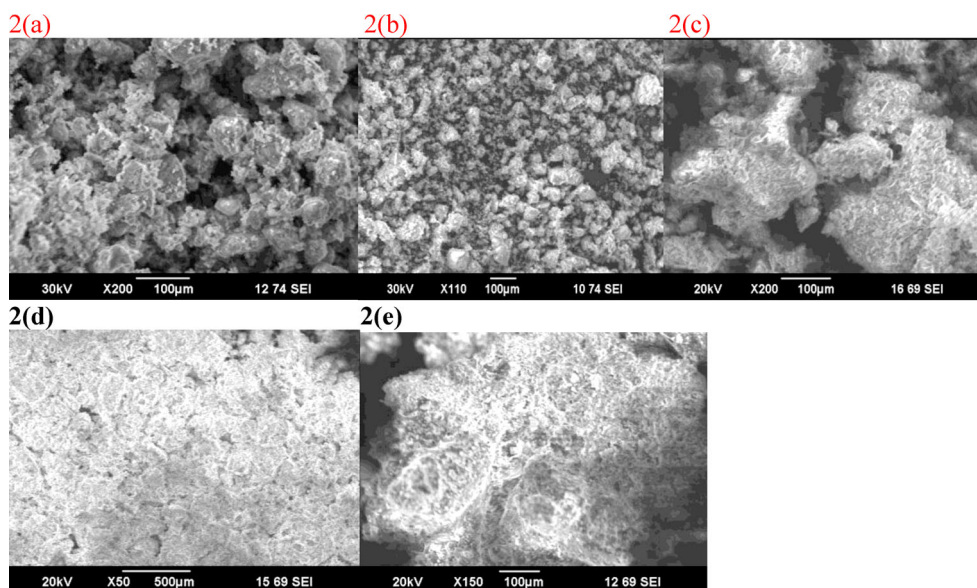


Figure 2. SEM images of $\text{GdCa}_4\text{O}(\text{BO}_3)_3$ doped with (a) Sm (b) Cu (c) Tb (d) Mn (e) Sb.

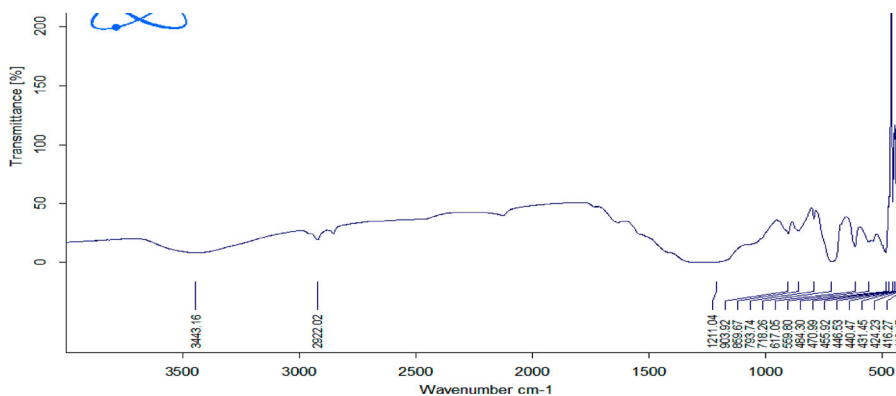


Figure 3. FTIR spectra of $\text{GdCa}_4\text{O}(\text{BO}_3)_3$.

structural rigidity to the materials. The luminescence properties of the materials are extremely influenced by non-bonded oxygen ions (non-bridging oxygen ions). There are four basic wave modes within the $(\text{BO}_3)_3$ cluster. Because of contaminants, the bands higher than 1500 cm^{-1} are O-H stretching vibrations. The bands within the $1200\text{--}1400\text{ cm}^{-1}$ range are created by uneven stretching modes of $(\text{BO}_3)_3$, whereas bands within the $850\text{--}1000\text{ cm}^{-1}$ range are caused by bilaterally symmetrical stretching modes of $(\text{BO}_3)_3$. Uneven and bilaterally symmetrical bending modes of $(\text{BO}_3)_3$, on the opposite hand, are found within the $600\text{--}750\text{ cm}^{-1}$ and $530\text{--}650\text{ cm}^{-1}$ ranges, severally.

External vibrations caused by wave and translational movement of $(\text{BO}_3)_3$, non-bridging element atoms, and translational motions of Ca^{2+} particle are shown by the bands below 500 cm^{-1} . The band appeared at around 424 cm^{-1} in our case is in step with the band at 418 cm^{-1} of non-bridging element ions rumored by Maczka et al. (39, 40).

3.4. Photoluminescence (PL) characterization

The single broad blue band peaking at 440 nm above the $^3P_{1,0} \rightarrow ^1S_0$ transitions of particle beneath 235 nm excitation is determined for $\text{GdCa}_4\text{O}(\text{BO}_3)_3: 0.1\text{mol}\%\text{Sb}$ shows a deep blue emission as shown in Figure 4. The excitation of blue emission is from the 1S_0 to 3P_1 transition, indicating the blue emissive self-trapped excitations originate only from 3P_1 level. The Sb dopant is thus the most excellent substance for receiving ready, blue phosphor materials (41).

The emission spectrum (Figure 5) of $\text{GdCa}_4\text{O}(\text{BO}_3)_3: 0.2\text{mol}\%\text{Mn}$ for 365 nm excitation shows intense broadband peaking at 543 nm, which can be assigned to $^4T_1 \rightarrow ^6A_1$ transition of Mn ions with spectrum in the yellow/orange range depending on the concentration of dopants. The shoulder peak noted at around 546 nm is due to Mn \pm Mn phonon pair emission (42).

The 374 nm excitation composes of a series of sharp lines peaking at 491, 546, 587 and 624 nm over the 5D_4 to 7F_j ($j = 3,4,5,6$) changeovers of $\text{GdCa}_4\text{O}(\text{BO}_3)_3: 0.1\text{mol}\%\text{Tb}$ (Figure 6). The most intense emission line happens at 546 nm, the $^5D_4 \rightarrow ^7F_5$ transition of Tb ions. The

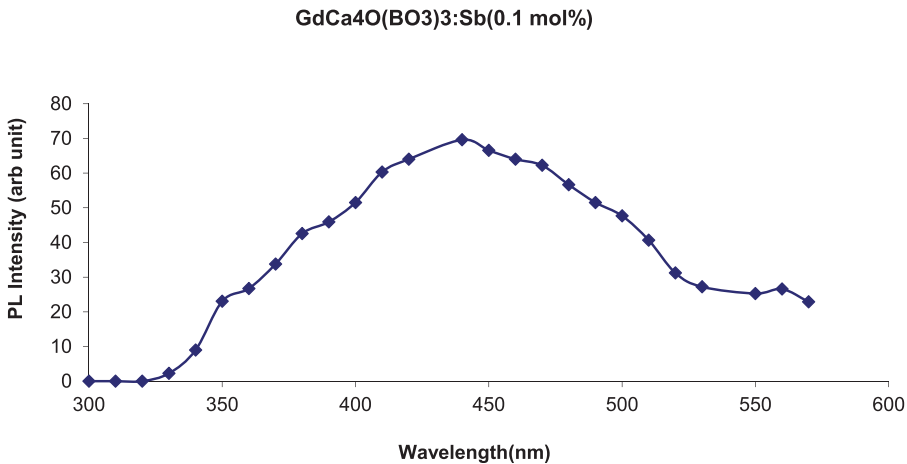


Figure 4. PL emission spectrum of $\text{GdCa}_4\text{O}(\text{BO}_3)_3:\text{Sb}$ (0.1 mol%).

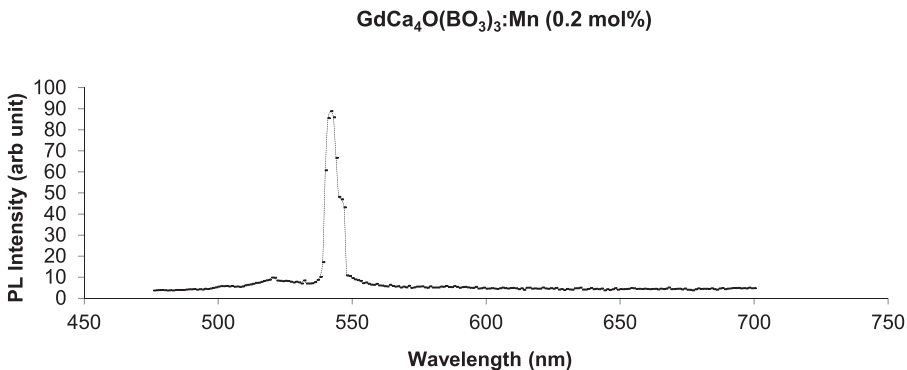


Figure 5. PL emission spectrum of $\text{GdCa}_4\text{O}(\text{BO}_3)_3:\text{Mn}$ (0.2 mol%).

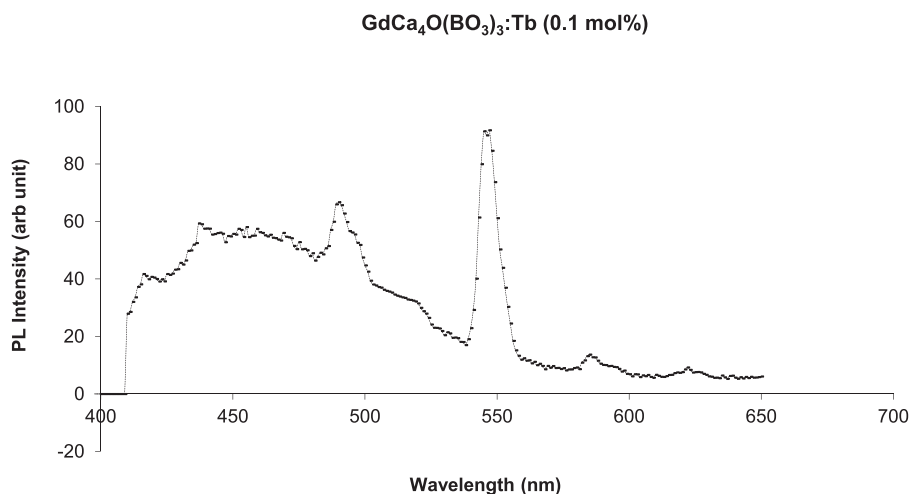


Figure 6. PL emission spectrum of GdCa₄O(BO₃)₃:Tb (0.1 mol%).

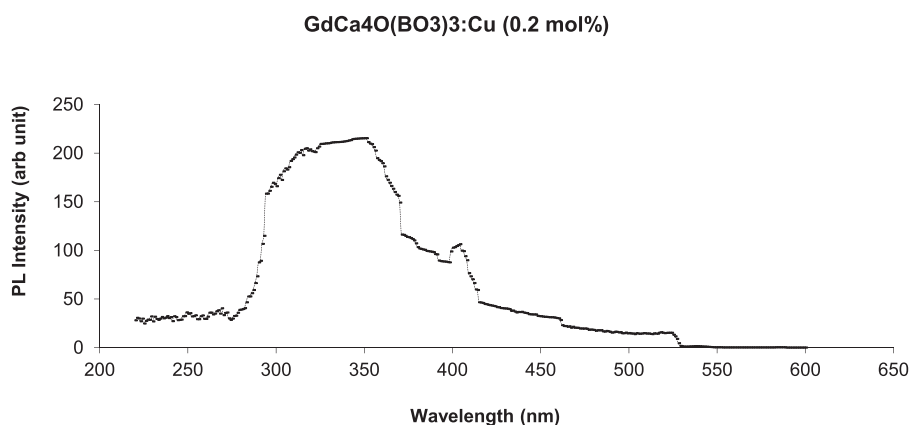


Figure 7. PL emission spectrum of GdCa₄O(BO₃)₃:Cu (0.2 mol%).

intensity of 491 and 546 nm lines, which correspond to the $^5D_4 \rightarrow ^7F_6$ transition of Tb³⁺ ions, is comparable and regarding a simple fraction of the intensity of the $^5D_4 \rightarrow ^7F_5$ line. The force of the emission lines 587 and 624 nm is fragile and matches the $^5D_4 \rightarrow ^7F_4$ and $^5D_4 \rightarrow ^7F_3$ transition of Tb³⁺ ions (43, 44).

The PL spectrum of GdCa₄O(BO₃)₃:Cu (0.2 mol%) exhibits broadband between 300 to 550 nm (Figure 7). The figure shows the emission spectra of the phosphor samples for Cu_{0.2mol%} with excitation at 247 nm. Emission peaks with terribly robust concentrations have twin bumps detected by 352 nm with 406 nm appointed to the $3d^94s^1 \leftrightarrow 3d^{10}$ transition in Cu⁺ ions unsettled to the presence of Cu luminescent centers in the oxiborate. The noted variation of emission may be due to energy transfer between Cu and the imperfections of oxiborate and hence causes luminescence. So this phosphor can be a favorable prospect for blue LED (45, 46).

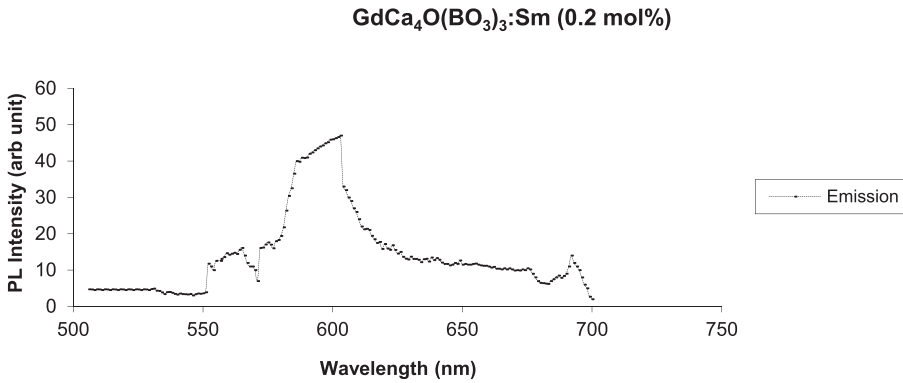


Figure 8. PL emission spectrum of GdCa₄O(BO₃)₃:Sm (0.2 mol%).

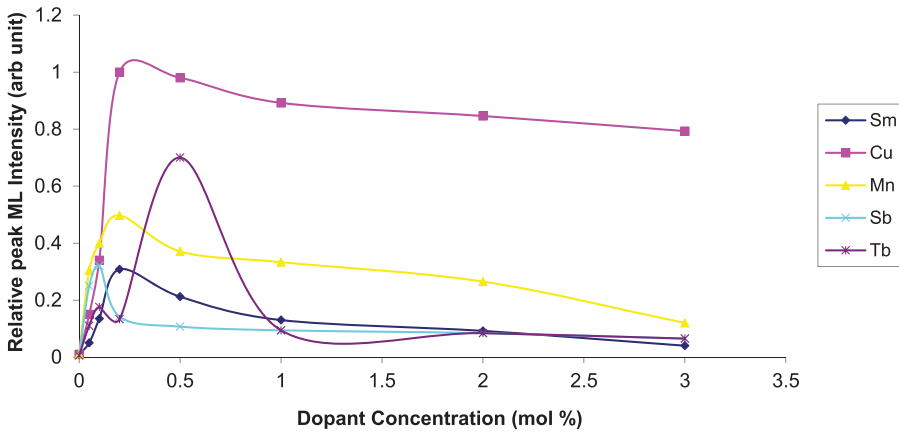


Figure 9. The consequence of dopant attentiveness on the peak ML intensity of GdCa₄O(BO₃)₃ sample.

Figure 8 illustrates the emission spectra of GdCa₄O(BO₃)₃ phosphor doped with Sm concentrations recorded at 405 nm excitation, which correspond to the absorption of the host and also the transition $^4G_{5/2} \rightarrow ^6H_{j/2}$ ($j = 5, 7, 9$) of Sm ions. Three characteristic emissions of Sm peaked at 566, 603 and 693 nm. The outstanding peak is noted at 603 nm as compared to the other two peaks. The peak observed at 566 nm is a magnetic dipole, while the peak at 603 nm is a slightly magnetic and a little bit a forced electric dipole transition (47).

The results obtained provide significant insight into understanding the PL processes and excited-state dynamics of the oxiborate phosphors. All the PL results of the present phosphor prove its worth in the field of solid-state lighting and LEDs applications.

3.5. Mechanoluminescence (ML) characterization

Peak ML intensity versus dopant concentration (0.05, 0.1, 0.2, 0.5, 1.0, 2.0, 3.0 mol%) for all the samples are revealed in Figure 9. The ML intensity is established to have relied

upon dopants application within the host $\text{GdCa}_4\text{O}(\text{BO}_3)_3$ sample. The ML intensity saturated at the different concentrations for various dopants ($\text{Cu}_{0.2\text{mol}\%}$, $\text{Mn}_{0.2\text{mol}\%}$, $\text{Tb}_{0.1\text{mol}\%}$, $\text{Sm}_{0.2\text{mol}\%}$, $\text{Sb}_{0.1\text{mol}\%}$) so concentration extinguishing occurs due to aggregation of dopant ions. Peak intensity at low dopant concentration within the host shows a decent property (cost-effective) for the event of radiation measure samples. Prominent ML intensity is recorded for $\text{GdCa}_4\text{O}(\text{BO}_3)_3:\text{Cu}_{0.2\text{mol}\%}$ phosphor.

ML glow curve of γ -irradiated $\text{GdCa}_4\text{O}(\text{BO}_3)_3$ sample for various dopants ($\text{Cu}_{0.2\text{mol}\%}$, $\text{Mn}_{0.2\text{mol}\%}$, $\text{Tb}_{0.1\text{mol}\%}$, $\text{Sm}_{0.2\text{mol}\%}$, $\text{Sb}_{0.1\text{mol}\%}$) and for various impact velocities (150, 200, 230, 280 cm/s) is shown in Figure 10(a–e). All the figures show isolated single peak altogether in the ready samples. It is determined that the ML intensity appeared when the impact of the load bore onto the sample. At the start, it is hyperbolic with time, reached its peak and so it

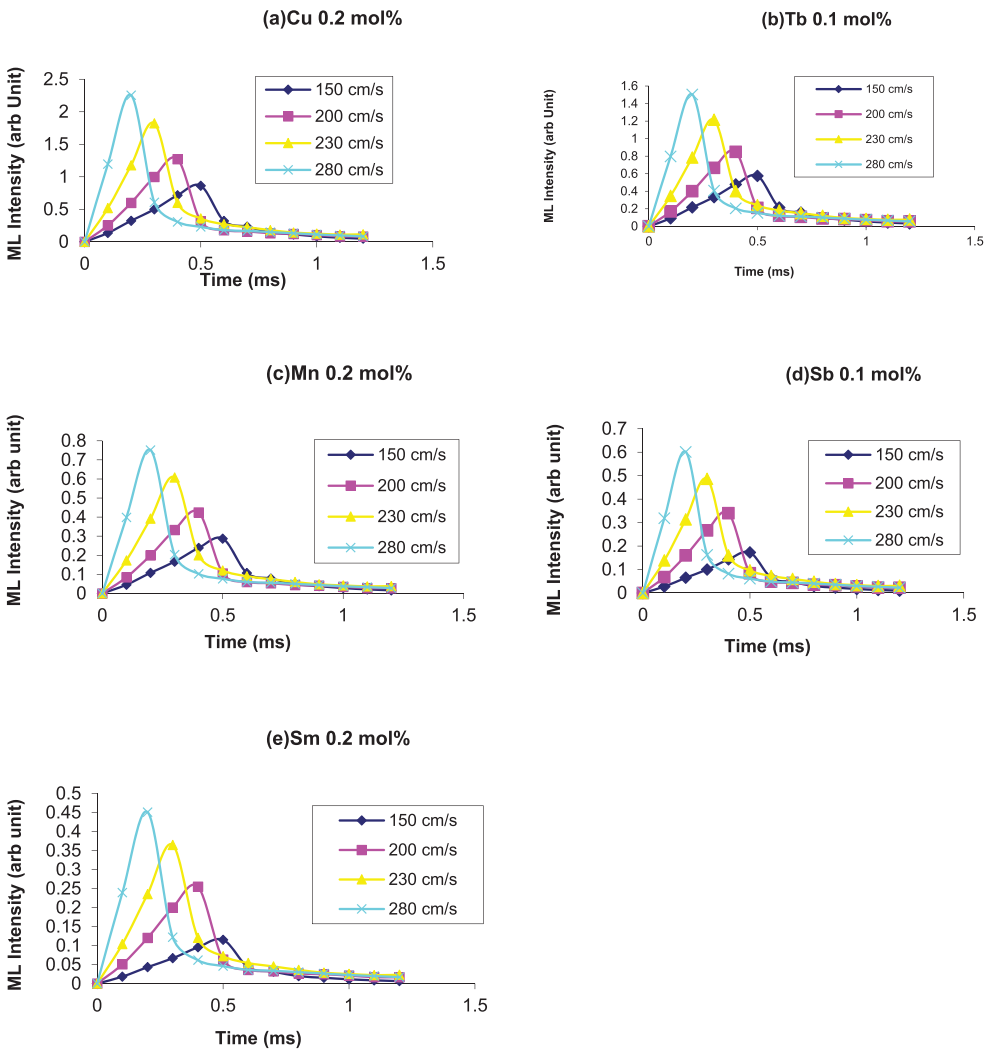


Figure 10. (a–e). Time dependence of ML intensity in the $\text{GdCa}_4\text{O}(\text{BO}_3)_3$ sample with different dopants at impact velocity ($150, 200, 230, 280 \text{ cm s}^{-1}$).

decayed. It is additionally determined that the height intensity will augment and shifted to for a shorter time with the rise of the impact speed.

When mechanical strain is functional to the sample, a possible distinction is produced because of the build-up of the electrical charge. Electricity equipment, a set of ferroelectric materials, exhibits the formation of a neighborhood charge departure called electrical dipoles because of their non-centrosymmetric crystal composition. With the rise of impact speed, the total ML intensity will increase indicating that a lot of range of active centers are created at higher impact. It is going to conjointly because of the creation of a new area (33–38). The shifting of peaks toward a shorter time urged that the interval of mechanical pulse slashed with higher impact speed, *i.e.* once an explicit compression additional it is tough to compress the sample (10–20, 48, 49).

Figure 11 illustrates that for higher standards of impact rate, the peak force of γ -irradiated $\text{GdCa}_4\text{O}(\text{BO}_3)_3$ sample for various dopants ($\text{Cu}_{0.2\text{mol}\%}$, $\text{Mn}_{0.2\text{mol}\%}$, $\text{Tb}_{0.1\text{mol}\%}$, $\text{Sm}_{0.2\text{mol}\%}$, $\text{Sb}_{0.1\text{mol}\%}$) enhanced virtually linearly with the impact rate.

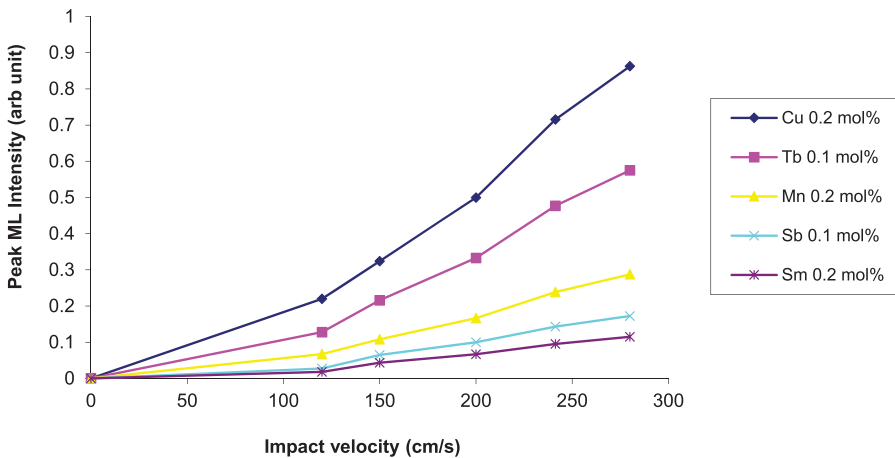


Figure 11. Dependence of peak ML intensity versus time curve of $\text{GdCa}_4\text{O}(\text{BO}_3)_3$ sample with dopants.

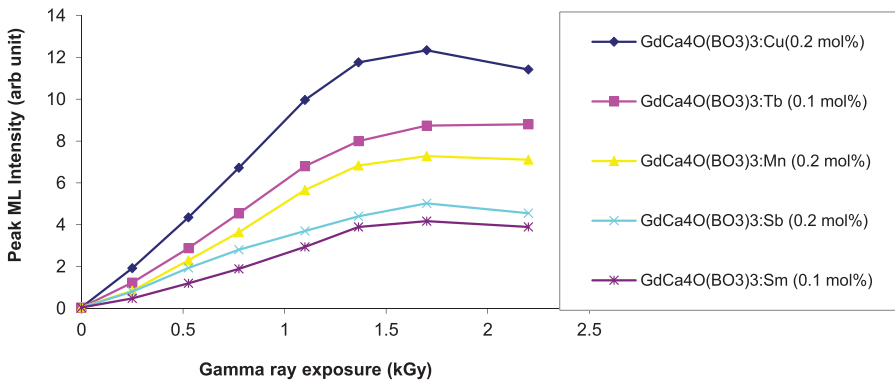


Figure 12. Variation of peak ML intensity with diverse γ -ray exposure of $\text{GdCa}_4\text{O}(\text{BO}_3)_3$ sample for different dopants ($\text{Cu}_{0.2\text{mol}\%}$, $\text{Mn}_{0.2\text{mol}\%}$, $\text{Tb}_{0.1\text{mol}\%}$, $\text{Sm}_{0.2\text{mol}\%}$, $\text{Sb}_{0.1\text{mol}\%}$).

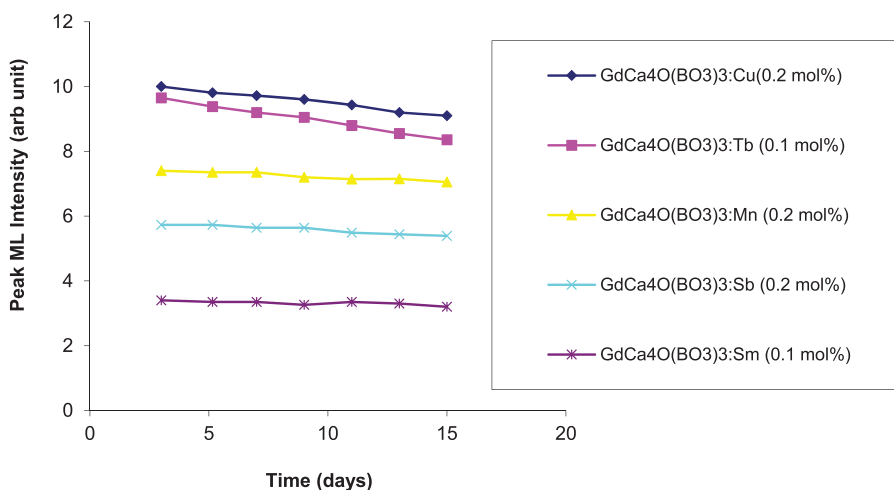


Figure 13. Dependence of peak ML intensity of $\text{GdCa}_4\text{O}(\text{BO}_3)_3$ sample for different dopants ($\text{Cu}_{0.2\text{mol}\%}$, $\text{Mn}_{0.2\text{mol}\%}$, $\text{Tb}_{0.1\text{mol}\%}$, $\text{Sm}_{0.3\text{mol}\%}$, $\text{Sb}_{0.2\text{mol}\%}$) on storage time.

Figure 12 explains the impact of γ -ray exposure to the peak ML intensity of $\text{GdCa}_4\text{O}(\text{BO}_3)_3$ sample for various dopants ($\text{Cu}_{0.2\text{mol}\%}$, $\text{Mn}_{0.2\text{mol}\%}$, $\text{Tb}_{0.1\text{mol}\%}$, $\text{Sm}_{0.2\text{mol}\%}$, $\text{Sb}_{0.1\text{mol}\%}$). The ML intensity linearly will increase up to 1.7 kGy then saturate for the next worth of γ -ray exposure. The boosting up in ML strength with increasing γ -ray dose may be owing to an increase in the number of active luminescent centers with γ -irradiation.

Figure 13 demonstrates the impact of storage in dark at the temperature on the peak ML intensities of γ -ray irradiated $\text{GdCa}_4\text{O}(\text{BO}_3)_3$ samples for a variety of dopants ($\text{Cu}_{0.2\text{mol}\%}$, $\text{Mn}_{0.2\text{mol}\%}$, $\text{Tb}_{0.1\text{mol}\%}$, $\text{Sm}_{0.2\text{mol}\%}$, $\text{Sb}_{0.1\text{mol}\%}$). It is seen that the weakening in ML intensity is incredibly low.

4. Conclusion

The $\text{GdCa}_4\text{O}(\text{BO}_3)_3$ with activators Cu, Mn, Tb, Sm, Sb are synthesized for various dopant concentrations by solid-state reaction technique and purity and crystallinity are confirmed by XRD of the host material. The FTIR measuring shows that $\text{GdCa}_4\text{O}(\text{BO}_3)_3$ has BO_3 group because of the essential structural elements in B-O triangles that provide constructional inflexibility of the substance. Non-bonded oxygen ions (non-bridging oxygen ions) strongly affect the luminescence properties of the material. The ML emission of $\text{GdCa}_4\text{O}(\text{BO}_3)_3$ samples for various dopants ($\text{Cu}_{0.2\text{mol}\%}$, $\text{Mn}_{0.2\text{mol}\%}$, $\text{Tb}_{0.1\text{mol}\%}$, $\text{Sm}_{0.2\text{mol}\%}$, $\text{Sb}_{0.1\text{mol}\%}$) is extremely vital for a tiny low variation in the impact velocities. The ready materials have low attenuation in ML on storage. ML performance of $\text{GdCa}_4\text{O}(\text{BO}_3)_3$ doped with Cu is most among all different dopants (Cu, Mn, Tb, Sm, Sb). $\text{GdCa}_4\text{O}(\text{BO}_3)_3\text{:Cu}_{0.2\text{mol}\%}$ presenting sensible linearity and intense ML. Furthermore, it is exposed that ready materials square measure less sensitive for a lower revelation of γ ray. It is also practical that ready materials are extremely less responsive for the lower exposure of γ ray. For that reason, the $\text{GdCa}_4\text{O}(\text{BO}_3)_3\text{:Cu}_{0.2\text{mol}\%}$ can be considered for stress sensing uses and accidental radiation dosimetry as Cu ion is an excellent activator for the preparation of the sensor-based ML material.

Disclosure statement

No potential conflict of interest was reported by the author(s).

Notes on contributors

Dr G. C. Mishra, MSc Physics, MPhil Physics, L.L.B. was born in Raigarh, C.G. He received his PhD degree in Physics in the field of Material Science from Central University Bilaspur, India. He is a Member of Luminescence Society of India, Indian Society for Particle Accelerators, Indian Physics Association and Indian Society for Technical Education. He has more than 25 years of experience of teaching and research. He received Gold Medal for MSc Physics University Merit list. Currently he is working as Professor of Physics & Asst. Dean School of Science, O P Jindal University, Raigarh. He is supervising PhD scholars and MSc students. He has published more than 50+ research papers in reputed international/national journals and conferences. He has been granted a PATENT recently. His main research interests involve Synthesis of LED phosphors, Mechanoluminescence, Lyoluminescence, Thermoluminescence, Photoluminescence characterization and uses of white phosphors in LED, Sensors and Dosimetry applications.

Upendra K. Verma, MPhil, Physics was born in Bhilai, CG. After completion of UG and PG degree from Kalyan College Bhilai Nagar, Chhattisgarh, he started his research work by getting admission in MPhil course at Guru Ghasi Das Vishwavidyalaya Bilaspur, Chhattisgarh. He started his career as a school teacher at DAV Public School Bilaspur and served for 13 years. On cracking Chhattisgarh Public Service Commission examination, he has been appointed as Assistant Professor in Physics at Government Dr. Indrajeet Singh College Akaltara. As on getting opportunity to teach in Higher Education he once again started his research work by getting registered in PhD course at O.P. Jindal University, Raigarh. He has been continuing his research work in the field of luminescence on the topic Synthesis and Characterization of doped and co-doped Phosphor. His main research interests involve Synthesis of LED phosphors, Mechanoluminescence, Lyoluminescence, Thermoluminescence, Photoluminescence characterization and uses of white phosphors in LED, Sensors and Dosimetry applications.

Prof. S. J. Dhoble obtained his MSc degree in Physics from Rani Durgavati University, Jabalpur, India in 1988. He obtained his PhD degree in 1992 in Solid State Physics from Nagpur University, Nagpur, India. Dr Dhoble is presently working as a Professor in the Department of Physics, Rashtrasant Tukadoji Maharaj Nagpur University, Nagpur, India. He has about 30 years of teaching at undergraduate and post graduate level and 29 years research experience. Consecutively in the years 2020 and 2021 Dr Dhoble stands among the 'Top 2% Scientists in the World' in the prestigious list published by a team of scientists in US' Stanford University. Best Research Award-2016, for the outstanding contribution in the field of research and related extenuation activity for the University, presented by R.T.M. Nagpur University, Nagpur, India on 5th Sept 2016. He is also a recipient of India's Top Faculty Research Award-2018 by Careers 360, for the top ten researchers in India in Physics. During his research career, he has worked on the synthesis and characterization of solid-state lighting materials and phosphors for solar cell efficiency enhancement, as well as development of radiation dosimetry phosphors and biosynthesis of nanoparticle and there applications. Dr Dhoble published 44 patents and few of them are already granted (Granted patents are 20: 01 South Korean, 01 South Africa, 13 Australian and 05 Indian). More than 757 research papers are published in Scopus indexing journals and his h-index is 39 and has 8901 citations on Scopus. Dhoble's citation on Google Scholar is 11034 and h-index is 43 and i10-index is 324. Dr Dhoble is an Editor of 'Luminescence: The Journal of Biological and Chemical Luminescence', John Wiley & Sons Ltd. Publication. He is also a Fellow of the Luminescence Society of India (LSI) and Fellow of Maharashtra Academic of Sciences (MASc).

References

- (1) Womack, F.N.; Goedeke, S.M.; Bergeron, N.P.; Hollerman, W.A.; Allison, S.W. *IEEE Trans. Nucl. Sci.* **2003**, *1*, 625.

- (2) Reynolds, G.T. *J. Lumin* **1997**, *75*, 295.
- (3) Chandra, B.P. Mechanoluminescence. In *Luminescence of Solids*; Vij D.R., Ed.; Springer, Boston, MA, **1998**; pp. 361–389.
- (4) Sweeting, L.M. *Chem. Mater.* **2001**, *13* (3), 854–870.
- (5) Bergeron, N.P.; Hollerman, W.A.; Goedeke, S.M.; Hovater, M.; Hubbs, W.; Finchum, A.; Moore, R.J.; Allison, S.W.; Edwards, D.L. *Int. J. Impact Eng.* **2006**, *33*, 91.
- (6) Xu, C.N.; Watanabe, T.; Akiyama, M.; Zheng, X.G. *Appl. Phys. Lett.* **1999**, *74*, 1236.
- (7) Xu, C.N.; Zheng, X.G.; Akiyama, M.; Nonaka, K.; Watanabe, T. *Appl. Phys. Lett.* **2000**, *76*, 179.
- (8) Akiyama, M.; Xu, C.N.; Matsui, H.; Nonaka, K.; Watanabe, T. *Appl. Phys. Lett.* **1999**, *75*, 2548.
- (9) Sage, I.; Badcock, R.; Humberstone, L.; Geddes, N.; Kemp, M.; Bourhill, G. *Smart Mater. Struct.* **1999**, *8*, 504.
- (10) Chandra, B.P.; Deshmukh, N.G.; Shrivastava, K.K. *Phys. Status Solidi.* **1986**, *96*, 167.
- (11) Chandra, V.K.; Chandra, B.P. *J. Lumin.* **2012**, *132* (3), 858–869.
- (12) Chandra, B.P.; Chandra, V.K.; Jha, P. *Phys. B* **2015**, *461*, 38–48.
- (13) Chandra, B.P.; Goutam, R.K.; Chandra, V.K.; Raghuvanshi, D.S.; Luka, A.K.; Baghel, R.N. *Radiat. Eff. Defects Solids* **2010**, *165*, 907.
- (14) Xu, C.N.; Watanabe, T.; Akiyama, M.; Zheng, X.G. *Appl. Phys. Lett.* **1999**, *74*, 2414.
- (15) Kim, J.S.; Kibble, K.; Kwon, Y.N.; Sohn, K.S. *Opt. Lett.* **2009**, *34*, 1915.
- (16) Kim, J.S.; Kibble, K.; Shin, N.; Sohn, K.S. *Acta Mater.* **2005**, *53*, 4337.
- (17) Kim, J.S.; Kwon, Y.N.; Shin, N.; Sohn, K.S. *Appl. Phys. Lett.* **2007**, *90*, 241916.
- (18) Chandra, B.P. *J. Lumin.* **2011**, *131*, 1203–1210.
- (19) Olawale, D.O.; Dickens, T.; Sullivan, W.G.; Okoli, O.I.; Sobanjo, J.O.; Wang, B. *J. Lumin.* **2011**, *131* (7), 1407–1418.
- (20) Ashish, T.; Khan, S.A.; Kher, R.S.; Mehta, M.; Dhoble, S.J. *J. Lumin.* **2011**, *131*, 1172–1176.
- (21) Li, J.; Hao, J.Q.; Zhang, C.X.; Tang, Q.; Zhang, Y.L.; Su, Q.; Wang, S. *Nucl. Instrum. Methods Phys. Res. B Beam Interact. Mater. Atoms* **2004**, *222*, 577.
- (22) Furetta, C.; Prokic, M.; Salamon, R.; Prokic, V.; Kitis, G. *Nucl. Instrum. Methods Phys. Res. Sect. A Accel. Spectrom. Detect. Assoc. Equip.* **2001**, *456*, 411–417.
- (23) Li, J.; Hao, J.Q.; Li, C.Y.; Zhang, C.X.; Tang, Q.; Zhang, Y.L.; Su, Q.; Wang, S.B. *Radiat. Meas.* **2005**, *39*, 229–233.
- (24) Furetta, C.; Kitis, G.; Weng, P.S.; Chu, T.C. *Nucl. Instrum. Methods Phys. Res. Sect. A Accel. Spectrom. Detect. Assoc. Equip.* **1999**, *420*, 441–445.
- (25) Liu, L.Y.; Zhang, Y.L.; Hao, J.Q.; Li, C.Y.; Tang, Q.; Zhang, C.X.; Su, Q. *Phys. Status Solidi A* **2005**, *202*, 2800–2806.
- (26) Liu, L.Y.; Zhang, Y.L.; Hao, J.Q.; Li, C.Y.; Tang, Q.; Zhang, C.X.; Su, Q. *Mater. Lett.* **2006**, *60*, 639–642.
- (27) Mishra, G.C.; Upadhyay, A.K.; Kher, R.S.; Dhoble, S.J. *J. Mater. Sci.* **2011**, *46*, 7275–7278.
- (28) Sahu, I.P.; Bisen, D.P.; Brahme, N. *J. Mater. Sci.: Mater. Electron.* **2016**, *27*, 3443–3455.
- (29) Mishra, G.C.; Upadhyay, A.K.; Dhoble, S.J.; Kher, R.S. *Micro Nano Lett.* **2011**, *12*, 978–981.
- (30) Mishra, G.C.; Dhoble, S.J.; Srivastava, A.; Dwiwedi, S.; Kher, R.S. *Optik.* **2018**, *158*, 826–830.
- (31) Norrestam, R.; Nygran, M.; Bovin, J.O. *Chem. Mater.* **1992**, *4*, 737–743.
- (32) Mishra, G.C.; Upadhyay, A.K.; Kher, R.S.; Dhoble, S.J. *J. Mater. Sci.* **2012**, *47*, 898–901.
- (33) Upadhyay, A.K.; Dhoble, S.J.; Kher, R.S. *Lumin. J. Biol. Chem. Lumin.* **2011**, *26*, 471–476.
- (34) Xu, C.N.; Watanabe, T.; Akiyama, M.; Zheng, X.G. *Appl. Phys. Lett.* **1999**, *74*, 2414–2416.
- (35) Akiyama, M.; Xu, C.N.; Taira, M.; Nonaka, K.; Watanabe, T. *Philos.Mag. Lett.* **1999**, *79*, 735–740.
- (36) Xu, C.N.; Zheng, X.G.; Akiyama, M.; Nonaka, K.; Watanabe, T. *Appl. Phys. Lett.* **2000**, *76*, 179–181.
- (37) Li, C.; Xu, C.N.; Yamada, H.; Imai, Y.; Zhang, H.; Zhang, L. *Key Eng. Mater.* **2008**, *368–372*, 401–1404.
- (38) Sohn, K.S.; Seo, S.Y.; Kwon, Y.N.; Park, H.D. *J. Am. Ceram. Soc.* **2002**, *85*, 712–714.
- (39) Barros, G.; Silva, E.N.; Ayala, A.P.; Guedes, I.; Loong, C.K.; Wang, J.; Hu, X.; Zhang, H. *Vib. Spectrosc.* **2008**, *46*, 100–106.
- (40) Małgczka, M.; Hanuza, J.; Pająłczkowska, A.; Morioka, Y.; van der Maas, J.H. *J. Raman Spectroscop.* **2004**, *35*, 266–273.
- (41) Xu, D.; Wei, R.; Cao, J.; Guo, H. *Opt. Mater. Express* **2017**, *7*, 2899–2904.
- (42) Shinde, K.N.; Nagpure, I.M.; Fulke, A.B.; Dhoble, S.J. *Luminescence* **2011**, *26* (5), 363–367.
- (43) Bajaj, N.S.; Omanwar, S.K. *J. Lumine* **2014**, *148*, 169–173.

- (44) Sailaja, S.; Dhoble, S.J.; Brahme, N.; Reddy, B.S. *J. Mater. Sci.* **2012**, *47*, 2359–2364.
- (45) McClure, D.S.; Weaver, S.C. *J. Phys. Chem. Solids* **1991**, *52*, 81–99.
- (46) Bhoyar, P.D.; Choithrani, R.; Dhoble, S.J. *Solid State Sci.* **2016**, *57*, 24–32.
- (47) Yerpude, A.N.; Dhoble, S.J. *J. Lumine* **2012**, *132*, 2975–2978.
- (48) Chandra, B.P.; Tutakane, P.R.; Verma, R.D.; Elyas, M. *Krist. Tech.* **1978**, *13*, 71–91.
- (49) Chandra, B.P.; Elyas, M. *Krist. Tech.* **1978**, *13*, 1341.